Proceedings of ASME Turbo Expo 2016: Turbomachinery Technical Conference and Exposition
GT2016
June 13 – 17, 2016, Seoul, South Korea

GT2016-58155

PASSIVE CONTROL OF CRITICAL SPEEDS OF A ROTATING SHAFT USING ECCENTRIC SLEEVES: MODEL DEVELOPMENT

A. J Kirk, J. Griffiths, C. Bingham, G. Knowles, R. Bickerton
School of Engineering
University of Lincoln
Lincoln, LN6 7TS, United Kingdom
email: akirk@lincoln.ac.uk, jgriffiths@lincoln.ac.uk, cbingham@lincoln.ac.uk,
gknowles@lincoln.ac.uk, rbickerton@lincoln.ac.uk

ABSTRACT

This paper considers the passive control of lateral critical speeds in high-speed rotating shafts through application of eccentric balancing sleeves. Equations of motion for a rotating flexible shaft with eccentric sleeves at the free ends are derived using the extended Hamilton Principle, considering inertial, non-constant rotating speed, Coriolis and centrifugal effects. A detailed analysis of the passive control characteristics of the eccentric sleeve mechanism and its impact on the shaft dynamics, is presented. Results of the analysis are compared with those from three-dimensional finite element simulations for 3 practical case studies. Through a comparison and evaluation of the relative differences in critical speeds from both approaches it is shown that consideration of eccentric sleeve flexibility becomes progressively more important with increasing sleeve length. The study shows that the critical speed of high-speed rotating shafts can be effectively controlled through implementation of variable mass/stiffness eccentric sleeve systems.

INTRODUCTION

To provide a practical focus to this study, the analysis presented in the paper considers industrial shaft machinery that rotates at high speed. Specifically, it considers sub-15MW industrial gas turbine units primarily for power generation or as mechanical prime movers. In order to prevent high vibration levels and consequent shutdowns, the engines are often operated at speeds below what would be normally considered as optimal. Indeed, Regulation API671 dictates that, in the case of a flexible coupling, the lateral safety margin should be at least 1.5 (that is, the lateral critical speed should be 1.5 times the operating speed) [1]. As a result of this requirement, critical speeds are often 'designed out' as part of the development process, suggesting that the source of the high vibrations levels lies elsewhere.

Figure 1. ECCENTRIC BALANCING SLEEVE

An attempt to address this problem has been reported by, Knowles *et. al* using an approach in which an eccentric balancing sleeve (Fig. 1) is retrofitted to existing coupling shafts [2,3].The design allows for a balance mass to be added to the shaft in such a way as to counter any residual unbalance that may exist. Fig 2 shows the balance corrections that are traditionally applied to the ends of the drive shaft are instead applied eccentrically by a pair of balancing sleeve arms. By this means, the trim balance mass applies a corrective centrifugal force to the drive shaft to limit the shaft end-reaction forces. The balancing sleeves are flexible by design therefore as well as increasing with speed, the correcting forces also increase in magnitude due to the increasing eccentric position of the flexibility of the sleeves. This mechanism therefore provides a means of amplifying the balance correction set at low speed. In addition, it also imparts a corrective bending moment to the drive shaft, which has a beneficial tendency to limit the shaft deflection. However, the successful operation of the design requires prior knowledge of the magnitude and position of the existing unbalance in the shaft in order to correctly set the magnitude of the trim balance masses required.

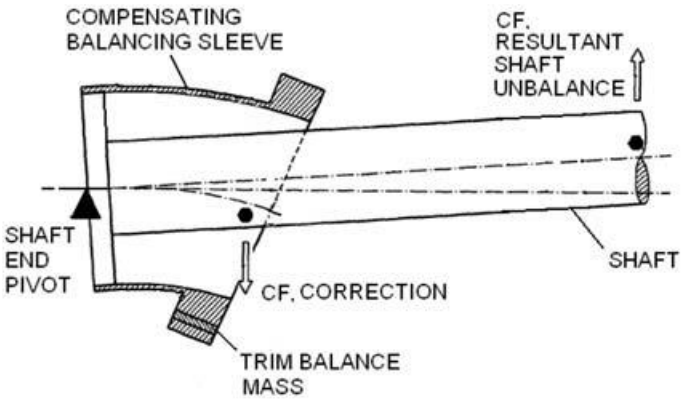

Figure 2. SCHEMATIC OF ECCENTRIC BALANCING SLEEVE

Practical problems with rotating shafts and rotors are usually reduced through appropriate design and careful balancing and alignment practices. However, it is not always possible to remove the source of vibration through these means, and in such cases mitigation techniques are employed viz. either active counteraction of the source of vibration or passive modification to the system by the addition of physical mass, damping or stiffness [6].

Active vibration control is a feedback control methodology in which an external actuator is used to modify the dynamic characteristics of the system. The effectiveness of active vibration control is heavily dependent on the robustness and response of the feedback system. Common systems include active bearings utilising magnetic or piezoelectric elements to achieve actuation [7-11].

Passive vibration control involves the modification of the physical mass, damping or stiffness of a system such as vibration isolation through anti-vibration mounting of supporting structures and introducing bearing damping through squeeze film dampers [10].

The eccentric balancing sleeve proposed by Knowles *et al.* is considered 'semi active', and allows for balancing across a wide speed range. However, by adding mass to the system in the form of a sleeve, the fundamental natural frequency can be changed, and hence the critical speed of the system will also change. Significant research is required to analyse the behaviour of the system due to the addition of the eccentric sleeves prior to embedding them into engines. From this analysis, additional passive control characteristics may be identified.

Here then, a detailed analysis of the passive control characteristics of the eccentric sleeve mechanism is conducted through the development, discretisation and solution of an approximated theoretical model and finite element simulation. Through comparison of the two models, the effect of varying the stiffness and mass of the eccentric sleeve on shaft critical speed, is investigated.

THEORETICAL MODEL

Fig.3 shows a linear-elastic, numerical model of a rotating shaft incorporating eccentric sleeves is derived and implemented in MATLAB. The model utilizes a rotating coordinate system to analyse a simplified shaft geometry with approximate cross-sectional areas and uniform material properties. Nonlinear terms arising from the derivation are neglected as a result of displacements being considered to be sufficiently small.

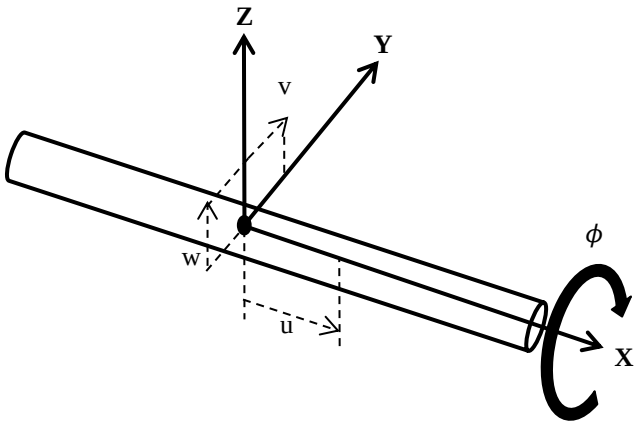

Figure 3. DISPLACEMENT AT POINT ON SHAFT

Due to the complex geometry of the eccentric sleeves, only their kinetic energy contribution is considered in the model i.e. accounting for mass/inertia and neglecting sleeve stiffness. Initial simulations by Kirk et al [12] showed that by considering the sleeves as rigid bodies made less than 1% difference in the determination of the critical speeds when compared with the flexible case.

In [12] the Extended Hamilton Principle and the derived individual variations of the kinetic and potential energies of the

system are used to obtain the equations of motion and associated boundary conditions. In the case of a constant rotational speed:

Axial Motion δu:

$$-m_0\ddot{u} + EAu'' = 0 \tag{1}$$

Y Lateral Bending δv:

$$\dot{\theta}^2 m_0 v + 2\dot{\theta} m_0 \dot{w} - m_0 \ddot{v} + \rho_0 I \ddot{v}'' - EIv'''' = 0 \tag{2}$$

Z Lateral Bending δw:

$$\dot{\theta}^2 m_0 w - 2\dot{\theta} m_0 \dot{v} - m_0 \ddot{w} + \rho_0 I \ddot{w}'' - EIw'''' = 0 \tag{3}$$

Torsion $\delta \phi$:

$$\dot{\theta}^2 (2\rho_0 I\phi) - 2\rho_0 I\ddot{\phi} + GI\phi'' = 0 \tag{4}$$

Strong boundary conditions arising from geometry of the problem:

$$\begin{aligned} u(0,t) &= u(L,t) = 0 \\ v(0,t) &= v(L,t) = 0 \\ w(0,t) &= w(L,t) = 0 \end{aligned} \tag{5 a-c}$$

Weak boundary conditions arising from the variational formulation:

x=0, $\delta v'$:

$$\begin{aligned} EIv'' - \Big(&\dot{\theta}^2\left(-I_{xx}v'(0,t) + I_{xy} + I_{xz}\phi(0,t)\right) \\ &- 2\dot{\theta}\left(I_{xx}\dot{w}'(0,t) + I_{xy}\dot{\phi}(0,t)\right) \\ &+ I_{yy}\ddot{v}'(0,t) + I_{yz}\ddot{w}'(0,t) \\ &+ I_{xx}\ddot{v}'(0,t) - I_{xz}\ddot{\phi}(0,t)\Big) \\ &- kv'(0,t) = 0 \end{aligned}$$

x =L, $\delta v'$:

$$\begin{aligned} -EIv'' - \Big(&\dot{\theta}^2\left(-I_{xx}v'(L,t) - I_{xy} - I_{xz}\phi(L,t)\right) \\ &- 2\dot{\theta}\left(I_{xx}\dot{w}'(L,t) - I_{xy}\dot{\phi}(L,t)\right) \\ &+ I_{yy}\ddot{v}'(L,t) + I_{yz}\ddot{w}'(L,t) \\ &+ I_{xx}\ddot{v}'(L,t) + I_{xz}\ddot{\phi}(L,t)\Big) \\ &- kv'(L,t) = 0 \end{aligned}$$

x =0, $\delta w'$:

$$\begin{aligned} EIw'' - \Big(&\dot{\theta}^2\left(-I_{xx}w'(0,t) - I_{xy}\phi(0,t) + I_{xz}\right) \\ &- 2\dot{\theta}\left(-I_{xx}\dot{v}'(0,t) + I_{xz}\dot{\phi}(0,t)\right) \\ &+ I_{yz}\ddot{v}'(0,t) + I_{zz}\ddot{w}'(0,t) \\ &+ I_{xx}\ddot{w}'(0,t) + I_{xy}\ddot{\phi}(0,t)\Big) \\ &- kw'(0,t) = 0 \end{aligned}$$

x =L, $\delta w'$:

$$\begin{aligned} -EIw'' - \Big(&\dot{\theta}^2\left(-I_{xx}w'(L,t) + I_{xy}\phi(L,t) - I_{xz}\right) \\ &- 2\dot{\theta}\left(-I_{xx}\dot{v}'(L,t) - I_{xz}\dot{\phi}(L,t)\right) \\ &+ I_{yz}\ddot{v}'(L,t) + I_{zz}\ddot{w}'(L,t) \\ &+ I_{xx}\ddot{w}'(L,t) - I_{xy}\ddot{\phi}(L,t)\Big) \\ &- kw'(L,t) = 0 \end{aligned}$$

x =0, $\delta\phi$:

$$\begin{aligned} GI\phi' - \Big(&\dot{\theta}^2\left(-I_{xy}w'(0,t) - I_{yy}\phi(0,t) + I_{xz}v'(0,t)\right. \\ &\left. - I_{zz}\phi(0,t)\right) \\ &- 2\dot{\theta}\left(-I_{xy}\dot{v}'(0,t) - I_{xz}\dot{w}'(0,t)\right) \\ &+ I_{xy}\ddot{w}'(0,t) + I_{yy}\ddot{\phi}(0,t) \\ &- I_{xz}\ddot{v}'(0,t) + I_{zz}\ddot{\phi}(0,t)\Big) = 0 \end{aligned}$$

x =L, $\delta\phi$:

$$\begin{aligned} -GI\phi' - \Big(&\dot{\theta}^2\left(I_{xy}w'(L,t) - I_{yy}\phi(L,t)\right. \\ &\left. - I_{xz}v'(L,t) - I_{zz}\phi(L,t)\right) \\ &- 2\dot{\theta}\left(I_{xy}\dot{v}'(L,t) + I_{xz}\dot{w}'(L,t)\right) \\ &- I_{xy}\ddot{w}'(L,t) + I_{yy}\ddot{\phi}(L,t) \\ &+ I_{xz}\ddot{v}'(L,t) + I_{zz}\ddot{\phi}(L,t)\Big) = 0 \end{aligned} \tag{6 a-f}$$

Discretisation

The equations of motion are discretised and dynamic system matrices formulated using the Galerkin method. Using method of weighted residuals, the mass and stiffness matrices take the form (7), (8) [13]:

$$\mathbf{k_{ij}} = \int_0^{\mathbf{L}} \boldsymbol{\phi}_\mathbf{i}\, \mathbf{L}\boldsymbol{\phi}_\mathbf{j}\mathbf{dx} \tag{7}$$

$$\mathbf{m_{ij}} = \int_0^{\mathbf{L}} \mathbf{m}\boldsymbol{\phi}_\mathbf{i}\boldsymbol{\phi}_\mathbf{j}\,\mathbf{dx} \tag{8}$$

Trial functions $\phi_i$and ϕ_j are spatial functions; $Y_i(x)$, $Y_j(x)$, $Z_i(x)$, $Z_j(x)$ and $\boldsymbol{\Phi}_i(x)$ corresponding to Y and Z bending and torsional displacements respectively. Approximate solutions for these are given in (9) to (11). The displacements function

solutions contain spatial ($\mathbf{Y_{i...}(x)}$) and time ($\mathbf{a_{v...}(t)}$) components and the corresponding eigenvectors($\mathbf{u_i}$).

$$v = \sum_{i=1}^{N} Y_i(x) a_v(t)\, u_i \tag{9}$$

$$w = \sum_{i=1}^{N} Z_i(x) a_w(t)\, u_i \tag{10}$$

$$\phi = \sum_{i=1}^{N} \Phi_i(x) a_\phi(t)\, u_i \tag{11}$$

Suitable admissible functions for the displacement functions are of the form $\sin\frac{i\pi x}{L}$ or $\cos\frac{i\pi x}{L}$ [14]. Chosen admissible functions must satisfy the strong boundary conditions of the shaft from (5). The discretised equations of motion are collated into the form (12). The system matrices are given in the Appendix with the individual components including mass and stiffness terms for the shaft, effects due to Coriolis and centrifugal forces, terms due to the influence of the eccentric sleeves and torsional spring effects of the flexible elements. In its simplest form, (12) can be converted into two first order differential equations (13) where M, C and K are the global system mass, stiffness and damping matrices, respectively [11].

$$\begin{aligned}([\mathbf{M_{sh}}] + [\mathbf{M_{sl}}])\{\ddot{\mathbf{q}}(\mathbf{t})\} \\ + ([\mathbf{C_{corsh}}] + [\mathbf{C_{corsl}}])\{\dot{\mathbf{q}}(\mathbf{t})\} \\ + ([\mathbf{K_{sh}}] + [\mathbf{K_T}] + [\mathbf{K_{centsh}}] \\ + [\mathbf{K_{centsl}}])\{\mathbf{q}(\mathbf{t})\} = \mathbf{0}\end{aligned} \tag{12}$$

$$\begin{bmatrix} C & M \\ M & 0 \end{bmatrix} \frac{d}{dt}\begin{Bmatrix} q(t) \\ \dot{q}(t) \end{Bmatrix} - \begin{bmatrix} K & 0 \\ 0 & -M \end{bmatrix}\begin{Bmatrix} q(t) \\ \dot{q}(t) \end{Bmatrix} \tag{13}$$

MATLAB is now readily used to obtain an eigenvalue solution for the system at chosen values of rotational speed. The number of terms in the Galerkin solution is empirically chosen to be nine in this instance, to provide good convergence characteristics without significantly impacting on required computational overhead.

FINITE ELEMENT MODEL

A dynamic finite element model of the full rotating shaft and eccentric sleeve system has been developed in ANSYS Workbench (Version 15.0.7), Fig. 4. The model is fixed at each end to replicate connection to driving and driven equipment (Fig. 5). An appropriate meshing strategy was obtained using a convergence study.

A modal analysis identifies the natural frequencies, with Campbell diagrams used to obtain the critical speeds of the shaft within a specific range of operating frequencies. Results from the modal analysis are used to visualise the mode shapes of the system.

Figure 4. FINITE ELEMENT MODEL OF SHAFT-SLEEVE SYSTEM

To investigate the effect of sleeve flexibility on the dynamics of the system, the geometry of the eccentric sleeves is removed and replaced with a point mass with equivalent inertia properties, as shown in Fig. 5.

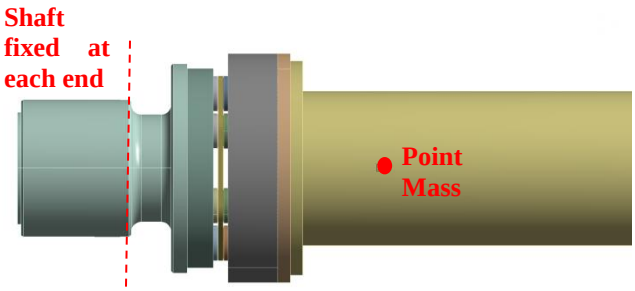

Figure 5. FINITE ELEMENT MODEL OF SHAFT WITH POINT MASS REPLACING SLEEVE

RESULTS

In order to assess the effect of sleeve stiffness, the critical speeds for the rotating shaft have been obtained for four eccentric sleeve configurations viz. no sleeve, short sleeve, medium sleeve and long sleeve. The different lengths were chosen in advance of experimental testing.

Fig.'s 6 and 7 show the normalised Campbell diagrams for the theoretical and ANSYS finite element models for the first bending mode of the shaft in each case, normalised against the maximum frequency and rotational speed. The natural frequencies of the system have been obtained in a rotating coordinate system; the critical speeds are determined by the speed at which the frequency of the mode becomes zero [15].

Table 1 gives the normalised critical speeds for each sleeve configuration for all three model variants. The critical speeds for each sleeve configuration are normalised with respect to the critical speed of the system with no sleeve attached.

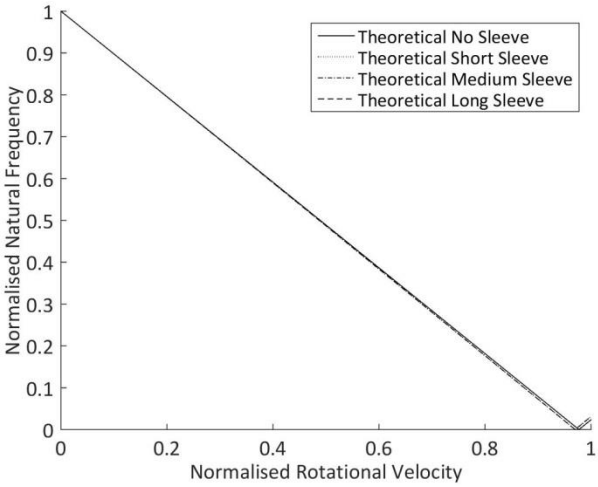

Figure 6. CAMPBELL DIAGRAM FOR THEORETICAL SOLUTION

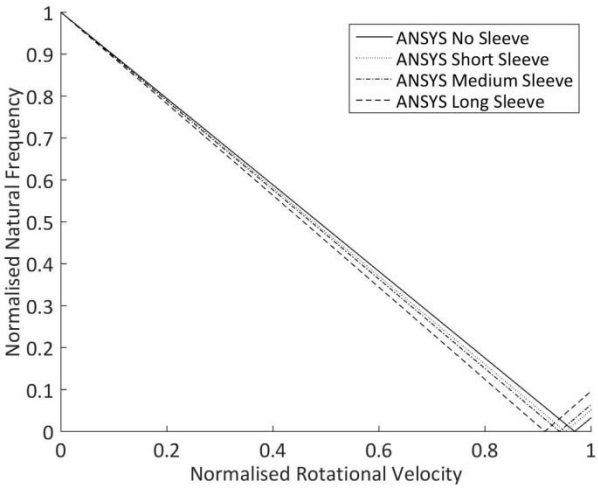

Figure 7. CAMPBELL DIAGRAM FOR FINITE ELEMENT MODEL

Table 1. NORMALISED CRITICAL SPEEDS

	No sleeve	Short	Medium	Long
Theoretical	1.000	0.9924	0.9923	0.9922
ANSYS	1.000	0.982	0.971	0.942
ANSYS Point Mass	1.000	0.991	0.989	0.987

DISCUSSION

Comparison of the Campbell diagrams and results in Table 1 show a disparity in the relative change of critical speed between the two models. The theoretical model shows a marked decrease in critical speed with the addition of the short sleeve but no further significant change with the addition of sleeves of increasing length. By contrast, the finite element model shows a continuing decrease in critical speed with the addition of sleeves of increasing length. This can be attributed to the theoretical model only considering the mass/inertia effects of the sleeves, as opposed to the finite element model which accounts for the full geometry of the system. As such, the results presented in Table 1 suggest that mass/inertia effects alone are not sufficient to describe the change in critical speed as eccentric sleeve length is increased. This follows a degree of intuition, where by increasing mass and reducing stiffness the natural frequencies of the system will decrease.

The effect of increasing sleeve length on stiffness can be readily observed in the mode shapes of the system under free vibration, as shown in Fig.'s 8 to 10. For the short sleeve, the deflection of the sleeve is roughly equal to that at the same point on the shaft; essentially it is rigid. However, as the length of the sleeve is increased, the deflection becomes significantly greater than that of the shaft at the same point. This can be rationalized by considering that, as the sleeve increases in length, it becomes more flexible. When considered in conjunction with the normalized critical speeds presented in Table 1, this indicates that sleeve flexibility becomes progressively more influential on the dynamics of the system as sleeve length increases.

Figure 8. FINITE ELEMENT OBTAINED FIRST BENDING MODE OF SHAFT WITH SHORT SLEEVE

Figure 9. FINITE ELEMENT OBTAINED FIRST BENDING MODE OF SHAFT WITH MEDIUM SLEEVE

Figure 10. FINITE ELEMENT OBTAINED FIRST BENDING MODE OF SHAFT WITH LONG SLEEVE

The effect of sleeve flexibility can be shown through the described modifications to the finite element model. Removing the sleeve geometry, the mass of the sleeve is induced on the system without any stiffness effects. Fig. 11 shows the normalised Campbell diagram for the ANSYS finite element model with point mass replacement. The normalised critical speeds are included in Table 1.

The results for the point mass finite element model are comparable to those of the theoretical model. There is an initial decrease in critical speed with the addition of the short sleeve but no further significant with the addition of the medium and long sleeves.

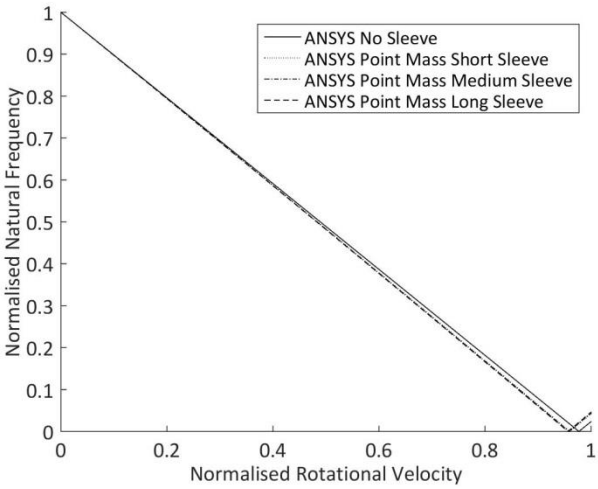

Figure 11. CAMPBELL DIAGRAM FOR FINITE ELEMENT MODEL WITH POINT MASSES

Removal of the sleeve geometry has shown that mass alone does not explain the alteration in critical speed and that sleeve stiffness does have a significant impact upon the dynamics of the shaft; this is opposed to the initial assumptions made in previous work [12]. This is an interesting result, given that the each sleeve is connected to the shaft at one end and in free space at the other. Although the overall mass of the system has been increased, the stiffness of the sleeve does not directly affect the stiffness of the shaft and would not be expected to alter the natural frequency significantly. This suggests that in free vibration, the flexibility of the sleeves is imparting a bending moment upon the shaft, thus altering its natural frequencies. The mechanism of passive control is therefore similar to the designed trim balancing method.

CONCLUSION

A detailed analysis of an eccentric sleeve mechanism for the passive control of the critical speeds of a rotating shaft has been conducted. The addition of an eccentric balancing sleeve to a rotating shaft has been shown to change the critical speed of the shaft. Through modification of the mass and stiffness characteristics of the system, the natural frequencies are reduced.

An approximated theoretical model and finite element simulation has been developed and used for the investigation. The modelling practices have identified potential bounds of applicability for the proposed model. When the eccentric sleeves possess high stiffness, the theoretical model can be used to accurately determine the critical speed of the shaft. However, the magnitude of influence of sleeve stiffness on the change of critical speed of the shaft increases with decreasing sleeve stiffness. As such, the accuracy of the theoretical model is reduced in the latter case, requiring the use of more complex finite element simulations, at the expense of incurring significant computation overhead.

With the stiffness of the sleeve identified as a key parameter, it is now possible to conduct a parametric study in order to find variations of mass and stiffness that offer optimal passive control of shaft critical speeds.

NOMENCLATURE

$\dot{\theta}$	Rotational velocity
m_0	Mass per unit area of shaft
ρ_0	Density of shaft
E	Young's modulus of shaft
G	Shear modulus of shaft
I	Second moment of area of shaft
L	Length of shaft
k	Stiffness of flexible element
x	Axial position along shaft length
u, v, w	Shaft displacements
ϕ	Torsional displacement
I_{xx}	Inertia coefficients of sleeves
Φ_i	Trial function for torsional displacement
M	Global mass matrix
K	Global stiffness matrix
C	Global damping matrix
M_{sh}	Shaft mass matrix
M_{sl}	Sleeve mass matrix
C_{corsh}	Shaft Coriolis force matrix
C_{corsh}	Sleeve Coriolis force matrix
K_{sh}	Shaft stiffness matrix
K_T	Element torsional stiffness matrix
K_{centsh}	Shaft centrifugal stiffness matrix
K_{centsl}	Sleeve centrifugal stiffness matrix
$q(t)$	Global displacement vectors

ACKNOWLEDGMENTS

The work presented in this paper is supported and financed by Siemens Industrial Turbomachinery Limited, Lincoln, United Kingdom.

REFERENCES

[1] American Petroleum Institute, 2007. "AQPI Standard 617 – Special Purpose Couplings for Petroleum, Chemical and Gas Industry Services".

[2] Kirk, A., Knowles, G., Stewart, J. and Bingham, C., 2013. "Mathematical development and modelling of a counter balance compensating sleeve for the suppression of lateral vibrations in high speed flexible couplings". ASME Turbo Expo 2013, 3-7 June 2013, San Antonio, Texas, USA.

[3] Knowles, G., Kirk, A., Stewart, J., Bickerton, R. and Bingham, C., 2014. "Theoretical investigation into balancing high-speed flexible shafts, by the use of a novel compensating balancing sleeve". Proceedings of the Institution of Mechanical Engineers, Part C: Journal of Mechanical Engineering Science, 228 (13). pp.2323-2336.

[4] Abduljabbar, Z., ElMadany, M.M. and AlAbdulwahab, A.A., 1996. "Active vibration control of a flexible rotor". Computers & Structures, 58 (3). pp.499-511.

[5] Palazzolo, A.B., Lin, R.R., Alexander, R.M., Kascak, A.F. and Montague, J.,1991. "Test and theory for piezoelectric actuator active vibration control of rotating machinery". Journal of Vibration and Acoustics, 113(2). pp.167-175.

[6] Wang, Y.A. and Inman, D., 2011. "Comparison of Control Laws for Vibration Suppression Based on Energy Consumption". Journal of Intelligent Material Systems and Structures, 22. pp.795-809.

[7] Zhou, S. and Shi, J., 2001. "Active Balancing and Vibration Control of Rotating Machinery: A Survey". The Shock and Vibration Digest, 33. pp.361-37.

[8] Burrows, C.R., Keogh, P.S. and Sahinkaya, M.N., 2009. "Progress towards smart rotating machinery through the use of active bearings". IMechE Part C: J Mechanical Engineering Science, 223. pp.2849-2859.

[9] Pinte, G., Devos, S., Stallaert, B., Symens, W., Swevers, J. and Sas, P., 2010. "A piezo-bearing for the active structural acoustic control of rotating machinery". Journal of Sound and Vibration, 329(9). pp.1235-1253

[10] Adams Jr, M.L, 2010. *Rotating machinery vibration. Second ed.* CRC Press.

[11] Friswell, M., Penney, J., Garvey, S. and Lees, A., 2010. *Dynamics of rotating structures*. Cambridge University Press

[12] Kirk, A., Georgiades, F. and Bingham, C., 2014. "Towards Determination of Critical Speeds of a Rotating Shaft with Eccentric Sleeves: Equations of Motion".Proceedings of the 9th IFToMM International Conference on Rotor Dynamics. Volume 21 of the series Mechanisms and Machine Science. pp.1809-1822.

[13] Meirovitch, L., 1980. *Computational methods in structural dynamics*. Sijthoff and Noordhoff. Alphen aan den Rijn, The Netherlands. pp. 301-305

[14] Suherman,S. and Plaut,R.H., 1997. "Use of a Flexible Internal Support to Suppress Vibrations of a Rotating Shaft Passing Through a Critical Speed". Journal of Vibration and Control, 3. pp.213-233

[15] Vollen, A. and Komzsik,L., 2012. *Computational Techniques of Rotor Dynamics with the Finite Element Model*. CRC Press. Boca Raton, FL

APPENDICES

APPENDIX 1 – SYSTEM MATRICES

$[\mathbf{M}_{sh}]$= Shaft Mass Matrix

$$\begin{bmatrix} -m_0[A_{ij}] - \rho I[B_{ij}] & 0 & 0 \\ 0 & -m_0[A_{ij}] - \rho I[B_{ij}] & 0 \\ 0 & 0 & -2\rho I[D_{ij}] \end{bmatrix}$$

$[K_{sh}]$ = Shaft Stiffness Matrix

$$\begin{bmatrix} -EI[C_{ij}] & 0 & 0 \\ 0 & -EI[C_{ij}] & 0 \\ 0 & 0 & -GI[E_{ij}] \end{bmatrix}$$

$[K_T]$= Torsional Element Stiffness

$$\begin{bmatrix} -k\left(\left[F_{L_{ij}}\right] + \left[F_{0_{ij}}\right]\right) & 0 & 0 \\ 0 & -k\left(\left[F_{L_{ij}}\right] + \left[F_{0_{ij}}\right]\right) & 0 \\ 0 & 0 & 0 \end{bmatrix}$$

$[K_{centsh}]$ = Shaft Centrifugal Force Matrix

$$\dot{\theta}^2 \begin{bmatrix} m_0[A_{ij}] & 0 & 0 \\ 0 & m_0[A_{ij}] & 0 \\ 0 & 0 & 2\rho I[D_{ij}] \end{bmatrix}$$

$[C_{corsh}]$= Shaft Coriolis Matrix

$$2\dot{\theta} \begin{bmatrix} 0 & m_0[A_{ij}] & 0 \\ -(m_0[A_{ij}]) & 0 & 0 \\ 0 & 0 & 0 \end{bmatrix}$$

$[\mathbf{M}_{sl}]$ = Sleeve Mass Matrix

$$-\begin{bmatrix} (I_{yy}+I_{xx})\left(\left[F_{0_{ij}}\right]+\left[F_{L_{ij}}\right]\right) & I_{yz}\left(\left[F_{0_{ij}}\right]+\left[F_{L_{ij}}\right]\right) & I_{xz}\left(\left[G_{L_{ij}}\right]-\left[G_{0_{ij}}\right]\right) \\ I_{yz}\left(\left[F_{0_{ij}}\right]+\left[F_{L_{ij}}\right]\right) & (I_{zz}+I_{xx})\left(\left[F_{0_{ij}}\right]+\left[F_{L_{ij}}\right]\right) & I_{xy}\left(\left[G_{0_{ij}}\right]-\left[G_{L_{ij}}\right]\right) \\ I_{xz}\left(\left[H_{L_{ij}}\right]-\left[H_{0_{ij}}\right]\right) & I_{xz}\left(\left[H_{0_{ij}}\right]-\left[H_{L_{ij}}\right]\right) & (I_{yy}+I_{zz})\left(\left[I_{0_{ij}}\right]+\left[I_{L_{ij}}\right]\right) \end{bmatrix}$$

$[\boldsymbol{C}_{corsl}]$ = Shaft Coriolis Matrix

$$2\dot{\theta}\begin{bmatrix} 0 & I_{xx}\left(\left[F_{L_{ij}}\right]+\left[F_{0_{ij}}\right]\right) & -I_{xy}\left(\left[G_{L_{ij}}\right]-\left[G_{0_{ij}}\right]\right) \\ -\left(I_{xx}\left(\left[F_{L_{ij}}\right]+\left[F_{0_{ij}}\right]\right)\right) & 0 & -I_{xz}\left(\left[G_{L_{ij}}\right]-\left[G_{0_{ij}}\right]\right) \\ -I_{xy}\left(\left[H_{0_{ij}}\right]-\left[H_{L_{ij}}\right]\right) & -I_{xz}\left(\left[H_{0_{ij}}\right]-\left[H_{L_{ij}}\right]\right) & 0 \end{bmatrix}$$

$[\boldsymbol{K}_{centsl}]$ = Sleeve Centrifugal Force Matrix

$$\dot{\theta}^2\begin{bmatrix} I_{xx}\left(\left[F_{L_{ij}}\right]+\left[F_{0_{ij}}\right]\right) & 0 & -I_{xz}\left(\left[G_{L_{ij}}\right]-\left[G_{0_{ij}}\right]\right) \\ 0 & I_{xx}\left(\left[F_{L_{ij}}\right]+\left[F_{0_{ij}}\right]\right) & -I_{xy}\left(\left[G_{0_{ij}}\right]-\left[G_{L_{ij}}\right]\right) \\ -I_{xz}\left(\left[H_{0_{ij}}\right]-\left[H_{L_{ij}}\right]\right) & -I_{xy}\left(\left[H_{L_{ij}}\right]-\left[H_{0_{ij}}\right]\right) & (I_{yy}+I_{zz})\left(\left[I_{0_{ij}}\right]+\left[I_{L_{ij}}\right]\right) \end{bmatrix}$$

APPENDIX 2 – SYSTEM SUB-MATRICES

MATRIX	ELEMENTS	VALUE	MATRIX	ELEMENTS	VALUE
$[A_{ij}]$	$i=j$ (Diagonal)	$\frac{L}{2}$	$[F_{0_{ij}}]$	ALL	$\frac{ij\pi^2}{L^2}$
	$i\neq j$ (Off diagonal)	0	$[F_{L_{ij}}]$	$i=j$	$\frac{ij\pi^2}{L^2}$
$[B_{ij}]$	$i=j$	$\frac{ij\pi^2}{2L}$		$i\neq j$	$\cos i\pi \cos j\pi \left(\frac{ij\pi^2}{L^2}\right)$
	$i\neq j$	0	$\left[G_{0_{ij}}\right]$	ALL	$\frac{j\pi}{L}$
$[C_{ij}]$	$i=j$	$\frac{i^2j^2\pi^4}{2L^3}$	$\left[G_{L_{ij}}\right]$	ALL	$\cos i\pi \cos j\pi \left(\frac{j\pi}{L}\right)$
	$i\neq j$	0	$\left[H_{0_{ij}}\right]$	ALL	$\frac{i\pi}{L}$
$[D_{ij}]$	$i=j$	$\frac{L}{2}$	$\left[H_{L_{ij}}\right]$	ALL	$\cos i\pi \cos j\pi \left(\frac{i\pi}{L}\right)$
	$i\neq j$	0	$\left[I_{0_{ij}}\right]$	ALL	1
$[E_{ij}]$	$i=j$	$\frac{ij\pi^2}{2L}$	$\left[I_{L_{ij}}\right]$	ALL	$\cos i\pi \cos j\pi$
	$i\neq j$	0			